PERFORMANCE OF A SINGLE EFFECT LIBR-WATER ABSORPTION CHILLER OPERATING WITH A MEMBRANE-BASED MICROCHANNEL ABSORBER

de Vega M.*, García-Hernando N. and Venegas M.
*Author for correspondence
ISE Research Group, Department of Thermal and Fluids Engineering,
Universidad Carlos III de Madrid,
Leganés, 28911,
Spain,
E-mail: mdevega@ing.uc3m.es

ABSTRACT

The simulation of a LiBr-H_2O absorber using a porous fiber for the heat and mass transfer between the liquid solution and the refrigerant vapour is considered. Heat and mass transfer processes are modeled by means of selected correlations and data gathered from the open literature. For the case considered in this study, the absorber channels are 5 cm length. We evaluate the ratio between the volume of the absorber and the cooling capacity in a complete chiller, producing a reduction in size in the order of 1.5 times the usual values found in falling film absorption using conventional shell and tubes heat exchangers.

The simulated membrane absorber is integrated in a single effect lithium bromide–water absorption chiller which performance is evaluated. The variable parameters are the external driving temperatures: final temperature in the desorber, the cooling temperature of the external fluid in the absorber and the condenser and the evaporating temperature.

The coefficient of performance (COP) obtained varies from 0.5 to 0.8 for cooling duties ranging between 4 W and 7 W. The chiller response to different circulated solution mass flow rates is also presented.

INTRODUCTION

The interest for small-scale absorption chillers in buildings and dwellings air-conditioning appliances has increased in the last years, coupled with the use of solar thermal systems as a way to reduce the electricity consumption in these applications. The absorber is one of the most performance limiting and volume demanding components of this kind of technology. The main challenge in designing and operating these devices is to maximize the mass transfer rate by getting as much interfacial area as possible, minimizing the overall size. This can be achieved using membrane contactors in microchannel heat exchangers. This new technology has already been considered for LiBr-H_2O and H_2O-NH_3 solution-refrigerant pairs. A review of membrane contactors applied in absorption refrigeration systems has been presented by Asfand and Bourouis [1]. In the present investigation, the LiBr-H_2O solution has been considered.

NOMENCLATURE

A	[m^2]	Area
c_P	[kJ/kgK]	Specific heat
D_e	[m^2/s]	Diffusion term
e	[m]	Thickness
h	[W/m^2K]	Convective heat transfer coefficient
i	[kJ/kg]	Specific enthalpy
J	[kg/m^2s]	Absorption rate
K	[m/s]	Mass transfer coefficient
k	[W/mK]	Thermal conductivity
l	[m]	Width
M	[kg/mol]	Molecular weight
m	[kg/s]	Mass flow rate
P	[Pa]	Pressure
q	[W]	Thermal power
R	[Pa.m^2s/kg]	Mass transfer resistance
T	[ºC]	Temperature
U	[W/m^2ºC]	Global heat transfer coefficient

Special characters

ρ	[kg/m^3]	Density

Subscripts

b	Solution boundary layer
cw	Cooling water
lv	Liquid-vapour
m	Membrane
ov	Overall
s	Solution
sat	Saturation
v	Vapour
va	Absorbed vapour

Membrane based absorbers use a microporous polymeric membrane at the solution-refrigerant vapour interface. Compared with conventional absorption devices there are several advantages of using microporous fiber modules for vapour absorption. These include larger interfacial area per unit volume, independent control of vapour and liquid flow rates, easier scale up, modular design and compactness.

Isfahani and Moghaddam [2] experimentally tested a microchannel absorber using a nanofibrous membrane, while Yu et al. [3] showed with a numerical simulation that several folds of enhancement in the absorption rate can be achieved with respect to conventional absorbers.

Following the simple model by Venegas et al. [4], we provide the values of the coefficient of performance of a complete absorption system working with this kind of micro absorber and the temperatures needed in the desorber for different operating conditions.

ABSORBER CONFIGURATION

In the absorber, the gaseous fluid (in the present case water vapour) passes the membrane and it is absorbed by the solution (LiBr-H_2O) flowing inside the constrained flow passages. The configuration considered for the absorber in the present study is shown in Figure 1. It is a plate-and-frame membrane module. It consists of a vapour channel, the contact membrane and the solution and cooling water channels separated by a metal wall.

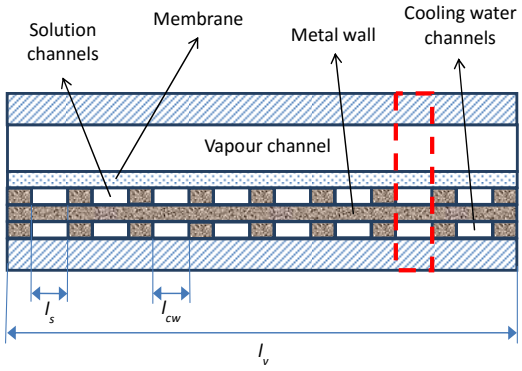

Figure 1 Membrane based absorber cross-section

In the membrane, many small diameter pores avoid mixing between vapour and solution. Surface tension prevents the solution from entering the holes, while the gas diffuses to the solution surface through the pores. The vapour pressure difference across the membrane is the driving force for vapour transfer. If the partial pressure of the vapour inside the solution is less than the vapour pressure, it is absorbed at the interface between solution and vapour.

The dimensions of the microchannels are in the present case: 150 μm height and 1.5 mm width. The length of the channels is 5 cm. We have considered a membrane 60 μm thick, with 0.8 porosity and a pore diameter of 1 μm. The number of water and solution channels is the same, equal to 13.

HEAT AND MASS TRANSFER MODELS

The microchannel absorber is divided in differential elements, as shown in Figure 2, where mass and energy balances are sequentially applied. The energy balance in the differential element *j* is written as:

$$(\dot{m}_{va}\, i_{lv})^j = q_S^j + q_v^j + q_{cw}^j \qquad (1)$$

Left term in equation (1) is the heat of absorption which is transferred to the solution, the vapour and the cooling water streams. Each of these terms can be calculated as:

$$q_S^j = (\dot{m}\cdot i)_S^{j+1} - (\dot{m}\cdot i)_S^j \qquad (2)$$

$$q_{cw}^j = \dot{m}_{cw}\, Cp_{cw}^j\, (T_{cw}^{j+1} - T_{cw}^j) = U_{s\_cw}^j A(T_s^j - T_{cw}^j) \qquad (3)$$

and

$$q_v^j = \left(\dot{m}\cdot i\right)_v^{j+1} - \left(\dot{m}\cdot i\right)_v^j = U_{s\_v}^j A(T_s^j - T_v^j) \qquad (4)$$

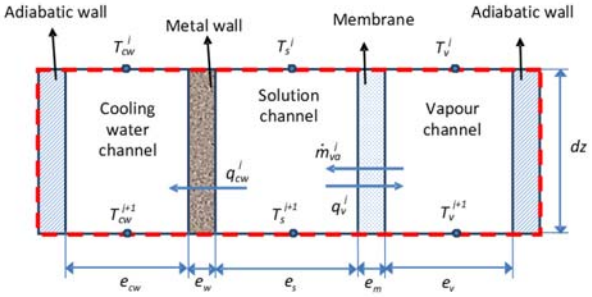

Figure 2 Differential control volume for heat and mass transfer balances

The global heat transfer coefficients in equations (3) and (4) are calculated as:

$$\frac{1}{U_{s\_cw}^j} = \frac{1}{h_{cw}^j} + \frac{e_w}{k_w^j} + \frac{1}{h_{s,cw}^j} \qquad (5)$$

$$\frac{1}{U_{s\_v}^j} = \frac{1}{h_v^j} + \frac{e_m}{k_m^j} + \frac{1}{h_{s,v}^j} \qquad (6)$$

The heat transfer coefficients (h) appearing in the overall coefficients U_{s_cw} and U_{s_v} in equations (5) and (6) have to be estimated using heat transfer correlations from the literature. In the present study we use the heat transfer correlations of Lee and Garimella [5] for the thermal entrance region and Shah and London [6] for fully developed flow, as described in [4].

The mass flow rate of vapour transported across the membrane is calculated taking into account the conditions of the bulk vapour and the bulk solution streams. For the differential element *j*, the absorbed mass flow rate is:

$$\dot{m}_{va}^j = J^j \cdot A = \frac{P_v - P_S^j}{R_{ov}^j} \cdot A \qquad (7)$$

P_v is the vapour pressure. P_s is the refrigerant partial pressure at the concentration and temperature of the bulk solution. The overall mass transfer resistance between the vapour and bulk solution (R_{ov}) includes the resistance to diffusion through the solution boundary layer (R_b) and the resistance to diffusion of vapour through the membrane active layer (R_m). The same approach presented by Ali [7] and applied in Venegas et al. [4] is followed here to obtain the overall mass transfer resistance:

$$R_{ov} = R_b + R_m = \frac{P_{sat}^j}{\rho_{ref}^j K_S^j} + \left[\frac{M}{e_m}\left(\frac{D_e}{RT_m}\right)\right]^{-1} \qquad (8)$$

In the first term of the right side, P_{sat} is the refrigerant saturated pressure at the bulk solution temperature, ρ_{ref} is the liquid refrigerant density and K_s is the mass transfer coefficient between the solution-vapour interface and the bulk solution. A suitable correlation for mass transfer in microchannels has not been found in the open literature. For this reason, the mass transfer coefficient of the solution K_s is calculated using mass and heat transfer analogy.

The last term in equation (8) corresponds to free molecular flow through the membrane. It is a function of the molecular weight of the vapour, M, the membrane thickness e_m and the temperature of the membrane, T_m. The diffusion term, D_e, is a function of the porosity, pore diameter and tortuosity of the membrane as in [4].

RESULTS AND DISCUSSION

The heat and mass transfer model described in the previous section has been implemented in Engineering Equation Solver software, EES™. Lithium bromide-water solution properties are calculated by EES with correlations developed by Patek and Klomfar [8], except viscosity and thermal conductivity calculated by EES using correlations provided by DiGuilio et al. [9]. EES uses the correlation of Harr et al. [10] for the thermodynamic properties of water. The transport properties are calculated using equations of the Electrical Research Association [11].

Absorber performance

The absorber has been simulated working with an inlet solution mass flow rate of 0.2 g/s at a concentration of 58% in LiBr. Different cooling water temperatures varying from 20ºC to 30ºC and two different evaporating temperatures are considered. In the presented results, the inlet solution temperature is fixed at 35ºC.

The difference in solution concentration between the inlet and the outlet of the absorber is shown in Figure 3.

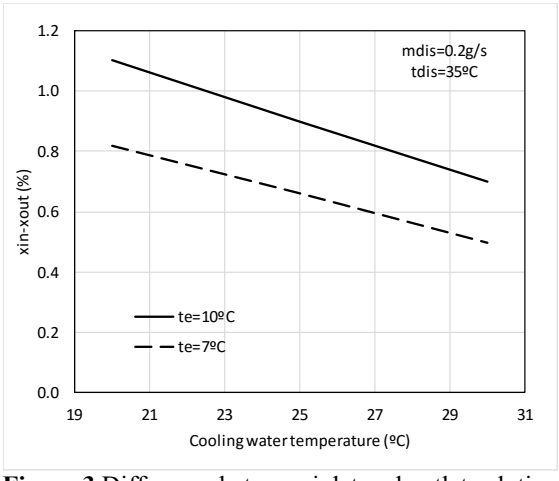

Figure 3 Difference between inlet and outlet solution concentration (x_{LiBr}) in the absorber

As could be expected, a higher difference in concentration is obtained when the cooling water temperature is lower. In this case, the absorption heat is more efficiently rejected and therefore the solution temperature is kept low. This is shown in Figure 4. In the simulation the inlet temperature to the desorber is kept constant. Therefore, the driving temperature difference for the absorption heat rejection is smaller at higher cooling temperatures. In this case, the temperature of the solution tends to increase, limiting the absorption process.

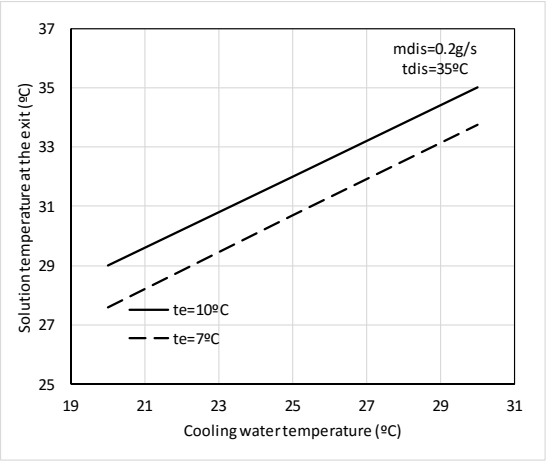

Figure 4 Solution temperature at the exit of the absorber

According to Figure 4, 10ºC increase in the cooling water temperature results in an increase of the solution outlet temperature of 6ºC.

The cooling effect that could be provided by the mass of vapour absorbed when the solution enters the absorber at 35ºC is shown in Figure 5.

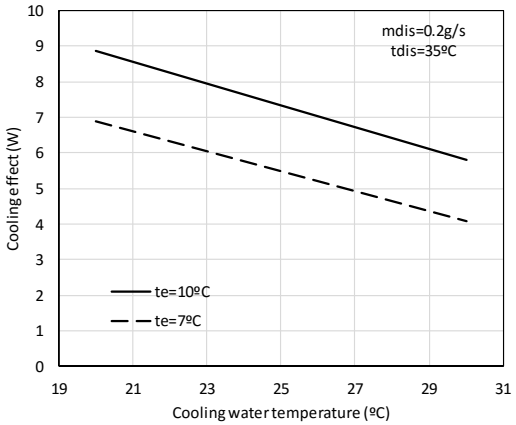

Figure 5 Cooling effect

The cooling effect varies between 4W and 9W. A change in the vapour temperature from 7ºC to 10ºC, implies an increase in the absorption capacity. As the main driving potential is the difference in pressure across the membrane this parameter is the decisive one in the performance of the absorber. In this way 2 W increase can be obtained with a 3ºC increase in the evaporation temperature.

For a given vapour temperature, i.e. vapour pressure, increasing the temperature of the cooling water leads to a lower absorption rate and, therefore, a lower cooling effect, at an approximate rate equal to -0.3 W/ºC.

The cooling effect relative to the volume of this membrane based absorber (calculated as the ratio between the cooling effect of the chiller equipped with it and the absorber volume, for the case analysed here -an absorber of 5 cm length), varies between 450 kW/m^3 in the worst case (highest cooling temperature and lowest evaporating pressure) to 950 kW/m^3 when operating at 10ºC in the evaporator with a cooling water temperature of 20ºC. For the LiBr-H_2O, this same parameter is 1.5 times lower using conventional shell and tubes falling film absorbers working with similar conditions [12]. Therefore, this membrane technology could be applied in low to medium cooling loads applications with smaller sizes than the conventional falling film absorbers. Moreover, the modular design of this type of heat exchanger can easily provide a proper scale up, which could allow even higher cooling effect to absorber volume ratios. For example, it could be easy to increase the capacity in such a way that the vapour and cooling water channels are shared by adjacent modules. In this way, this ratio can be increased almost twice.

Absorption cycle performance

The absorber has been studied operating in a complete absorption system, as the one depicted in Figure 6.

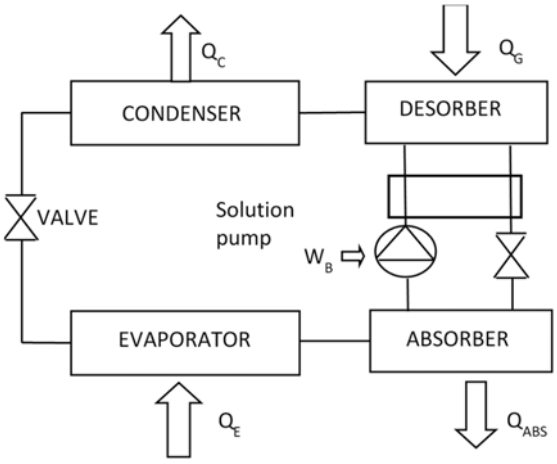

Figure 6 Absorption chiller

Input parameters employed in the simulation are the inlet conditions in the absorber: for the solution, temperature, concentration and mass flow rate; and temperature and mass flow rate for the cooling water. It has been considered that the same cooling water employed in the absorber is the water that cools the condenser. This will define the pressure in the condenser, which is the same as in the desorber. For the given inlet concentration at the absorber and the desorber pressure, the final vapour generation temperature is calculated. An example of such a cycle is depicted in Figure 7.

We have analysed the cycle working at an evaporation temperature of 7ºC. Different solution mass flow rates entering the absorber and cooling water temperatures have been considered and the complete thermodynamic cycle has been solved.

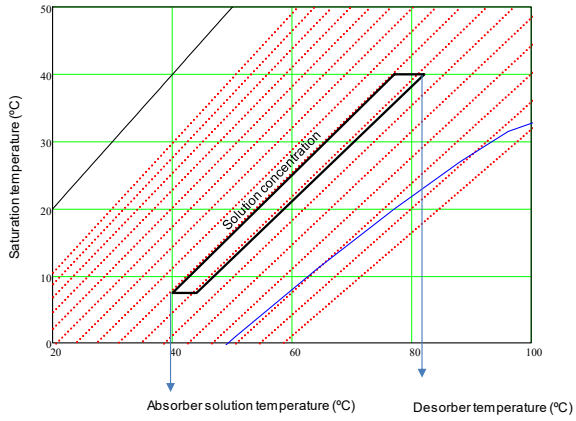

Figure 7 Thermodynamic cycle of the solution in a P-t-x diagram for the LiBr-H_2O solution

Figure 8 shows the solution temperature at the absorber outlet, for the different solution mass flow rates.

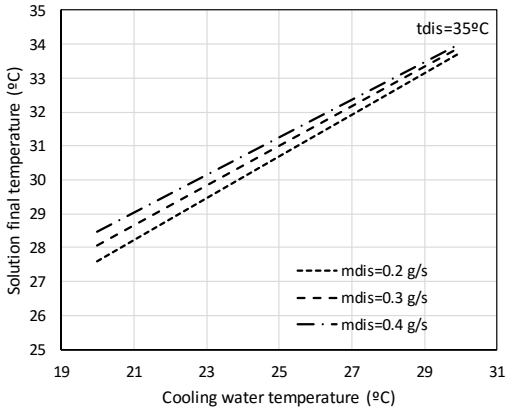

Figure 8 Solution temperature at the exit of the absorber

The cooling process is more effective at low solution mass flow rates and therefore the solution temperature is kept low, as shown in Figure 8. At higher cooling water temperatures, the influence of the solution mass flow rate in the heating of the solution tends to diminish.

The final temperature in the absorber determines the pressure in the desorber (as depicted in Figure 7). With this value, the final desorber temperatures are calculated. The results are shown in Figure 9. According to these results, lower mass flow rates at lower cooling water temperatures entail lower heating temperatures in the desorber. As shown with Figure 3, at low cooling water temperatures the outlet concentration decreases and therefore the corresponding pressure and desorber temperature are lower.

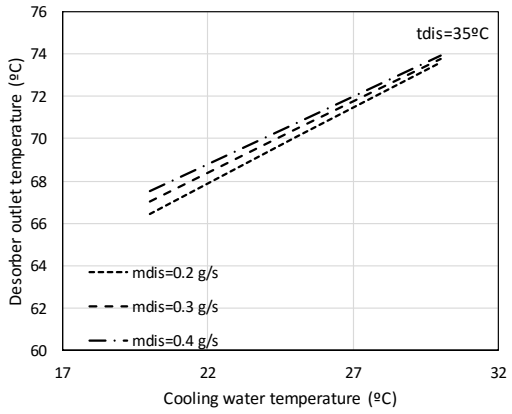

Figure 9 Desorber outlet temperature

The COP is calculated as the ratio between the cooling effect and the heat needed in the desorber. The results are shown in Figure 10.

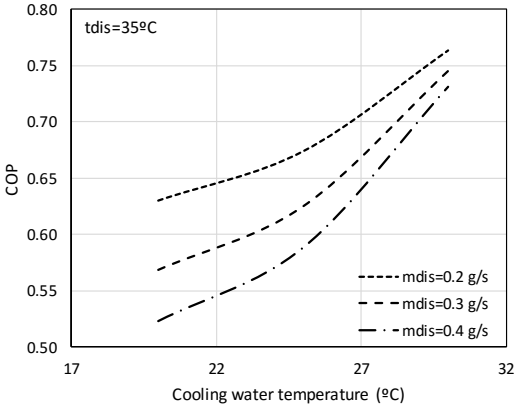

Figure 10 Coefficient of Performance

The values of the COP are similar to the ones found in conventional systems.

For a fixed cooling water temperature, the efficiency decreases with the increase of the solution mass flow rate. This effect is more pronounced at lower cooling temperatures (higher temperature difference between the solution and the cooling water). At these conditions, the solution temperature at the exit of the absorber is lower, and therefore the heat needed in the generator increases, giving a lower COP.

CONCLUSION

The use of a membrane based absorber with a volume of 10 cm^3 can provide a cooling effect of 9 W. This provides a cooling to volume ratio higher than the ones found in conventional absorbers, which could encourage the development of this kind of technology in low to medium applications.

The effect of the solution mass flow rate is important at low cooling water temperatures. This should be taken into account when operating at part load if this parameter is used as a controlling variable.

The operation of this type of absorber in a complete chiller can provide efficiency ratios similar to the ones found in conventional absorption systems.

Low cooling water temperatures improve the cooling effect, at a rate of 0.3W/ºC. In these conditions, low heating temperatures in the desorber are needed (below 70ºC), and solar thermal collectors could be used to supply the heat in the desorber.

REFERENCES

[1] Asfand F., Bourouis M., A review of membrane contactors applied in absorption refrigeration systems, *Renewable and Sustainable Energy Reviews,* Vol. 45, 2015, pp. 173-191.

[2] Isfahani RN, Moghaddam S., Absorption characteristics of lithium bromide (LiBr) solution constrained by superhydrophobic nanofibrous structures, *International Journal of Heat and Mass Transfer*, Vol. 63, 2013, pp. 82-90.

[3] Yu D, Chung J., Moghaddam S., Parametric study of water vapour absorption into a constrained thin film of lithium bromide solution, *International Journal of Heat and Mass Transfer*, Vol. 63, 2013, pp.82-90.

[4] Venegas M., de Vega M., García-Hernando N., Ruiz-Rivas U., A simple model to predict the performance of a H_2O-LiBr absorber operating with a microporous membrane, *Energy*, vol. 96, 2013, pp. 383-393.

[5] Lee P-S., Garimella SV., Thermally developing flow and heat transfer in rectangular microchannels of different aspect ratios, *International Journal of Heat and Mass Transfer,* 2006, Vol.49 pp. 3060-3067

[6] Shah RK., London AL., Laminar flow forced convection in ducts, in: A source book for compact heat exchanger analytical data, *Advances in heat transfer* Suppl 1. New York: Academic Press, 1978.

[7] Ali AHH., Design of a compact absorber with a hydrophobic membrane contactor at the liquid-vapor interface for lithium bromide-water absorption chillers, *Applied Energy*, Vol. 87, 2010, pp. 1112-1121

[8] Patek J., Klomfar J.A., A computationally effective formulation of the thermodynamic properties of LiBr-H2O from 273 to 500K over full composition range, *International Journal of Refrigeration*, Vol. 29, 2006, pp. 566-578.

[9] DiGuilio RM., Lee RJ., Jeter SM., Teja AS., Properties of Lithium bromide-water solutions at high temperatures and concentrations – I thermal conductivity, *ASRHAE Transactions*, RP-527, 1990, pp. 527-702-8.

[10] Harr L., Gallagher JS, Kell GS, NBS/NRC steam tables, *Hemisphere Publishing Co.*, 1984.

[11] Electrical Research Association Steam Tables, Thermodynamic properties of water and steam; viscosity of water and steam, thermal conductivity of water and steam, *Edward Arnold Publishers,* London, 1967.

[12] Kim KJ., Berman NS., Chau DSC., Wood BD., Absorption of water vapour into falling films of aqueous lithium bromide, *International Journal of Refrigeration*, Vol. 18, no.7, 1995, pp. 486-494.